Warehouse Commodity Classification from Fundamental Principles. Part I: Commodity & Burning Rates

M.J. Gollner[a,*], K. Overholt[b], F.A. Williams[a], A.S. Rangwala[b], J. Perricone[c]

[a] *University of California, San Diego, Dept. of Mechanical and Aerospace Engineering. 9500 Gilman Drive, La Jolla, CA 92093-0411.*
[b] *Worcester Polytechnic Institute, Department of Fire Protection Engineering. 100 Institute Road, Worcester, MA 01609-2280*
[c] *Creative FPE Solutions. 1242 Thomas Avenue, San Diego, CA 92109*

Abstract

An experimental study was conducted to investigate the burning behavior of an individual Group A plastic commodity over time. The objective of the study was to evaluate the use of a nondimensional parameter to describe the time-varying burning rate of a fuel in complex geometries. The nondimensional approach chosen to characterize burning behavior over time involved comparison of chemical energy released during the combustion process with the energy required to vaporize the fuel, measured by a B-number.

The mixed nature of the commodity and its package, involving polystyrene and corrugated cardboard, produced three distinct stages of combustion that were qualitatively repeatable. The results of four tests provided flame heights, mass-loss rates and heat fluxes that were used to develop a phenomenological description of the burning behavior of a plastic commodity. Three distinct stages of combustion were identified. Time-dependent and time-averaged B-numbers were evaluated from mass-loss rate data using assumptions including a correlation for turbulent convective heat transfer. The resultant modified B-numbers extracted from test data incorporated the burning behavior of constituent materials, and a variation in behavior was observed as materials participating in the combustion process varied.

*Corresponding author
Email address: mgollner@ucsd.edu (M.J. Gollner)

Variations between the four tests make quantitative values for each stage of burning useful only for comparison, as errors were high. Methods to extract the B-number with a higher degree of accuracy and future use of the results to improve commodity classification for better assessment of fire danger is discussed.

Keywords:
commodity classification, B number, Spalding number, warehouse fire, corrugated cardboard, polystyrene, group a plastic

---

Nomenclature

Symbols	
B	B-number (Spalding Mass Transfer Number, Equation 1) (-)
c_p	Specific Heat at Constant Pressure (J/kg K)
$\bar{h}$	Heat Transfer Coefficient (W/m^2 K)
ΔH_g	Heat of Gasification (J/kg)
ΔH_c	Heat of Combustion (J/kg)
k	Thermal Conductivity (W/m K)
$\dot{m}_f{}''$	Mass-Loss Rate (Mass Flux) (kg/m^{2}s)
Nu	Nusselt Number (-)
Pr	Prandtl Number (-)
$\dot{q}''$	Heat Flux (W/m^2)
r	Mass Consumption Number ($Y_{O_2}/\nu_s Y_{F,T}$) (-)
t	Time (s)
T	Temperature (K)
X_f	Flame Length (Height) (m)
X_p	Pyrolysis Length (Height) (m)
$Y_{F,T}$	Mass Fraction of Fuel in Transferred Phase (-)
Y_{O_2}	Mass Fraction of Oxygen (-)
y_f	Flame Standoff Distance (cm)
Greek Symbols	
α	Thermal Diffusivity (m^2/s)
ν_s	Stoichiometric Oxygen/Fuel Mass Ratio (-)
ρ	Density (kg/m^3)
ν	Kinematic Viscosity (m^2/s)
χ	Radiation Fraction, Equation 1 (-)
Subscripts	
g	Gas
∞	Ambient
f	Flame
p	Pyrolysis Region
Abbreviations	
ASTM	American Society for Testing and Materials
NFPA	National Fire Protection Association

1. Introduction

The storage of commodities in large warehouses poses a unique hazard to occupants, fire fighters, and surrounding communities due to the concentration of flammable, often toxic materials stored to heights of up to 16 meters (50 ft). A recent fire at Tupperware Brands Corp.'s manufacturing and distribution center in Hemingway, South Carolina has brought increased attention to the current need for improvement of large warehouse fire protection [1]. The fire was ignited by an electrical spark in a rack and quickly spread, completely destroying the 15,329 m^2 facility over a period of 35 hours. The warehouse was fully protected by in-rack sprinklers, installed to current codes and standards, yet the protection system still failed. A series of similar losses have occurred, as summarized in table 1.

Table 1: Recent Fire Losses in Large Warehouse Storage Facilities.

05/22/09	Furniture Warehouse– Houston, TX	4,600 m^2 warehouse, filled with furniture and electronics. An Inventory of $5 million was lost. 120 Fire Fighters were involved in putting the fire out [2].
12/11/07	Warehouse Fire– Hemingway, SC	15,329 m^2 warehouse storing plastic Tupperware. Warehouse was protected by sprinklers to code, 78 firefighters responded but fire burned out of control for a 35-hour period [1].
6/19/07	Furniture Warehouse Fire– Charleston, SC	9 firefighters died. Furniture presented much larger fire hazard than protection system could handle. Flashover occurred while firefighters were attempting to find the seat of the fire, after one employee was rescued. [3].
12/16/03	Furniture Warehouse Fire– NY	1 firefighter died while searching for the seat of a fire in a furniture and mattress warehouse [4].
3/14/01	Supermarket Fire– Phoenix, AZ	1 firefighter died. Fire began in storage pile in the rear of the store, spreading throughout the store rapidly via attic and duct space [5].
12/18/99	Paper Warehouse Fire– MS	1 firefighter died after becoming lost in a paper warehouse fire. The structure was equipped with a sprinkler system [6].
12/3/99	Cold-Storage and Warehouse Building Fire– MA	6 firefighters died after becoming lost in a six-floor, maze-like building searching for two victims. The building was abandoned at the time of the fire [7].
4/16/96	Lowes Store– Albany, GA	Fire grew so rapidly it penetrated the roof and filled the building with smoke down to the 1.5 m (5 ft) level, all within about 5 minutes. The fire took over 2 days to extinguish, destroying the 8,000 m^2 warehouse. The fire resulted from commodities stored in racks not matched to the fire hazard [8].

Current methods for commodity classification are outlined by FM Global and the National Fire Protection Association (NFPA) based upon full-scale rack storage tests of "standard" commodities. Standard commodities consist of a product, usually plastic, paper, or glass cups contained within a segregated corrugated cardboard box [9]. The classification scheme currently used in the United States places commodities into one of seven groups, Class I-IV general commodities or Group A-C plastic commodities. The Group A plastic commodity represents the greatest fire hazard. The scheme was developed from large-scale tests, comparing the performance of fire sprinklers with varying water application densities to control a fire in a large rack-storage configuration of commodities [10]. In general, stored commodities for warehouses undergo a variety of small-scale tests as an initial evaluation of their fire hazard, but for even moderately hazardous commodities, additional mid-to-large-scale testing is required at great expense [11]. Despite several previous studies, there does not currently exist a good method to correlate or compare small-scale test data to large-scale fire tests [12, 13]. Attempts to develop a large-scale model have also not addressed the fact that commodities and their packages involve several mixed materials, and the influence of these different materials together must be accounted for.

The stream of current large warehouse losses, shown in table 1 suggests changes to current warehouse design principles may be necessary to stem this current trend. An appropriate fundamental starting point for research, however, is difficult to determine. The burning rate, fire-spread rate, time to ignition, and fuel vaporization temperature are all factors that affect the burning of a fuel, but for a fire in a warehouse setting an adequate indication of flammability and suppression performance might well be determined solely from the burning rate of the commodity in the warehouse. While the critical heat flux and time to ignition are relevant in determining whether a fire will start, since the function of sprinklers protecting a facility is to control and suppress fires that occur, their requirements are influenced more strongly by the burning rate and spread rate, and spread rates may correlate with burning rates sufficiently well. Careful study of the small-scale burning rates of a standard Group A plastic commodity, therefore, was chosen for study. Because this commodity group represents the greatest hazard and because its large-scale behavior has been extensively studied, more data on its small-scale burning behavior may serve as a useful starting point for future investigations.

2. Definition of the B-number

It has been shown by Pagni and Shih [14] that upward laminar flame propagation can be described well by the B-number (also called Spalding's mass transfer number) [15]. The B-number appears in a boundary condition at the fuel surface in the classical Emmons solution for forced-flow flames over a condensed fuel [16]. This dimensionless parameter is quite simply a ratio that compares a summation of the various impetuses (e.g. heat of combustion) for burning to a summation of the various resistances (e.g. heat of vaporization) to the process. Originally [16] a purely thermodynamic quantity, its definition can be extended to encompass effects of different heat-transfer processes [17]. A useful definition that can be selected is [17]

$$B = \frac{(1-\chi)(\Delta H_c Y_{O_{2,\infty}})/\nu_s - c_{p,\infty}(T_p - T_\infty)}{\Delta H_g + Q} \tag{1}$$

where χ is the fraction of the total energy released by the flame that is radiated to the environment, ΔH_g denotes the heat of gasification of the condensed fuel and ΔH_c represents the heat of combustion. Here ν_s denotes the oxygen-fuel mass stoichiometric ratio, $Y_{O_2,\infty}$ is the mass fraction of oxygen in ambient air, $C_{p,\infty}$ represents the specific heat of air at an ambient temperature of T_∞, and T_p equals the pyrolysis temperature of the fuel. The parameter Q represents the normalized non-convective heat transfer at the surface, given by

$$Q = \frac{\dot{q}''_{s,c} + \dot{q}''_{s,r} - \dot{q}''_{f,r}}{\dot{m}''_f} \tag{2}$$

where $\dot{m}''_f$ is the burning rate per unit area, $\dot{q}''_{s,c}$ represents the rate of in-depth conduction of energy per unit area, $\dot{q}''_{s,r}$ represents the rate of surface re-radiation of energy per unit area, and $\dot{q}''_{f,r}$ denotes the radiative energy feedback from the flame to the surface per unit area. Thus, a large B-number basically implies a highly exothermic fuel relative to the heat required for gasification.

Some prior work has classified material flammability using a B-number specific to homogeneous materials [14, 18, 19]. A warehouse commodity however, consists of collections of different materials, and if a practical flammability ranking scheme is to be developed it should take into account the flammability of the basic product, its packaging, and its container. By experimentally determining the burning behavior of a mixed material, in this

work by determination of a modified B-number, a relative influence of mixed-material interactions and turbulence can be estimated for various stages of burning. In calculation of the B-number accuracy is sacrificed in favor of providing a description of the burning behavior throughout its combustion process. This is important in providing a qualitative picture of the small-scale burning behavior of commonly-used warehouse commodities, and is a stepping stone to design representative tests of higher accuracy. Because the B-number has been shown to predict the burning rate in simple geometries [14, 20], and thus the heat release rate, it arises as a relevant parameter to describe the thermal loading in a theoretical fire. This knowledge could be useful in a commodity ranking scheme because suppression systems are designed to control a potential thermal load created by stored materials, if adequate accuracy could be achieved while applying such a method to larger scales.

In warehouse protection "fire suppression" is typically defined as limiting fire spread long enough for fire crews to arrive and extinguish the fire, but definitions vary, and suppression also may be equated with providing extinction. Rasbash [21] has indicated that a critical B-number may be defined below which extinction occurs by water application. Thus, irrespective of whether extinction or delaying spread is the criterion, the B-number arises as a relevant parameter with potentially wide application to future studies.

3. Calculation of the B-number from Experiments

One approach to correlating the vaporization and combustion rates of a warehouse commodity is to follow the procedure presented by Kanury [22], which expresses the average burning rate per unit area $\dot{m}''_f$ as

$$\dot{m}''_f = \frac{\overline{h}}{c_{p,g}} \ln(B+1) \tag{3}$$

where $\bar{h}$ is the heat-transfer coefficient and $c_{p,g}$ may be approximated as the specific heat of air at a temperature equal to an average of flame temperature and ambient [23]. This equation links the burning rate, $\dot{m}''_f$ to the heat-transfer conditions $\overline{h}/c_{p,g}$ and material/thermodynamic $\ln(B+1)$ controlling parameters assuming a steady burning rate and constant $c_{p,g}$. As explained in a recent publication [24], a number of improved laminar boundary-layer types of theories lead to formulas that are more complicated than this, but

the results are qualitatively the same, and the fluctuating flames and incipient turbulence of the present experiments raises questions about the degree of applicability of such theories. For these reasons, this simplistic approach was chosen over other relevant approaches, to provide a more straightforward method of calculation.

To estimate the rate of convective heat transfer in our simplified approach, and thus the influence of the flow field during upward turbulent burning, a relation with the Nusselt number, Nu_x may be used [25], namely

$$\frac{\bar{h}}{c_g} = \frac{\rho_g \alpha_g}{X_p} \overline{\mathrm{Nu}_x} \tag{4}$$

where ρ_g and α_g are the density and thermal conductivity of air, respectively. From this an average heat-transfer coefficient, $\bar{h}$ is determined. The Nusselt number is determined from a standard correlation for turbulent convective heat transfer to a vertical surface [26]

$$\overline{\mathrm{Nu}_x} = 0.13(\mathrm{Gr}_x \mathrm{Pr})^{1/3} \tag{5}$$

where Gr_x is the Grashof number of the flow, and Pr is the Prandtl number of the gas, $\mathrm{Pr} = \nu_g/\alpha_g$. This correlation pertains to a flat, vertically oriented surface heated solely by convection heat transfer. With the Grashof number defined as

$$\mathrm{Gr}_x = \frac{g X_p^3 \Delta T}{\nu_g^2 T_g} \tag{6}$$

where $\Delta T = T_f - T_\infty$ equations 3–5 can be combined to yield the expression

$$B = \exp\left(\frac{\dot{m}_f{}''}{\rho_g \alpha_g 0.13 [g \Delta T / \nu_g \alpha_g T_g]^{1/3}} \right) - 1 \tag{7}$$

which can be used to calculate a B-number from experimental measurements. The flame temperature, T_f and relevant gas-phase properties are assumed to be approximately constant. Note that this expression for the B-number is dependent only on properties of the gas phase and the mass-loss rate; no fuel properties appear. The equation therefore becomes sensitive to measurements of mass-loss rate and burning surface area, incorporated in the term $\dot{m}_f{}''$. This approach is useful for experiments in which turbulent convective heat transfer dominates radiative feedback, as is estimated to occur in the

present experiments. Radiation, while not dominant in the present experiments does grow throughout the test duration, and therefore it does affect the measured value of $\dot{m}''_f$ to some extent at later stages. In the approach adopted here, this radiation effect is thus incorporated into an experimental effective B number, to be used with the convective heat-transfer correlation to describe the fire behavior. The absence of the length X_p in equation 7 is a special characteristic of natural convective heat transfer to vertical surfaces being dominant in the experiments. If radiation were dominant and convection negligible, then a different approach would be appropriate.

4. General Evolution of the Combustion

Figures 1 and 2 show a theoretical picture of the burning observed in a standard warehouse commodity. Figure 3 shows an illustrative representation of the burning behavior through these theoretical stages. The heat flux to unignited material from the fire plume that extends upward over the distance $(X_f - X_p)$ is responsible for the rapid upward spread of the flame. In figures 1 and 2 the length of the fire plume, $(X_f - X_p)$ is a function of the B-number and pyrolysis height [27].

During the early stages of the fire (figure 1), the flame is small, and the burning rate is a function only of the material properties of the corrugated board. This will be described as stage I of burning for a standard warehouse commodity. Heat flux from combustion pyrolyzes the board and packing material, releasing gaseous fuel adjacent to the combustion surface. Some of this fuel burns in the boundary layer in front of the fuel surface, but some is carried above its originating height and burns above, creating much larger flames. This fuel carried above its originating surface has been called *excess pyrolyzate* [14]. The pyrolysis height increases with time in the early stage represented by figure 1. In the second diagram of figures 1 and throughout the conditions of figure 2 it has reached the top of the commodity. This initial period is indicated in figure 3 as stage I.

Heat flux via in-depth conduction through the corrugated board can pyrolyze the packing material and commodity, releasing combustible vapors. As the outer corrugated board layers break down, these combustible vapors diffuse through the remaining board, enhancing the flame spread rate. At this stage, the B-number is a function of the material properties of the corrugated board as well as the pyrolysis vapor from the heated commodity that penetrates the corrugated board. As time advances, the corrugated board

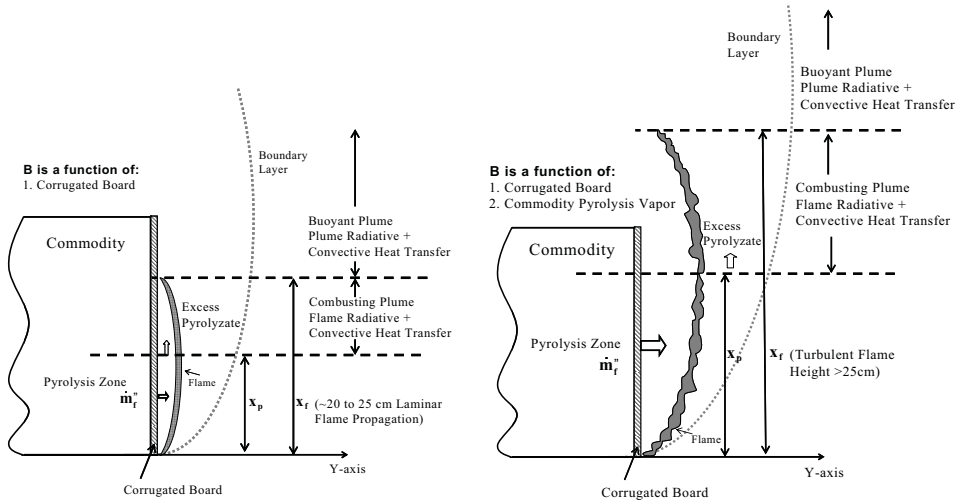

Figure 1: (Left) Flame propagation up the surface a warehouse commodity during the early stages of fire, where the flame height is below the height of the commodity. (Right) Flame height reaches above the height of the commodity. Both images are representative of Stage I burning of a standard plastic warehouse commodity.

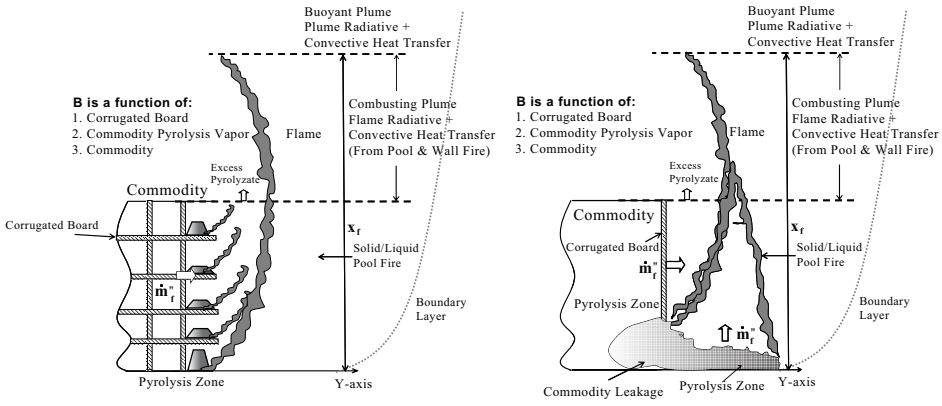

Figure 2: Turbulent upward flame propagation at later stages of the fire, where the commodity within the box either burns from within the box (left) or has spilled out into a pool fire (right). The commodity is now in stage III of burning where plastic dominates the burning rate.

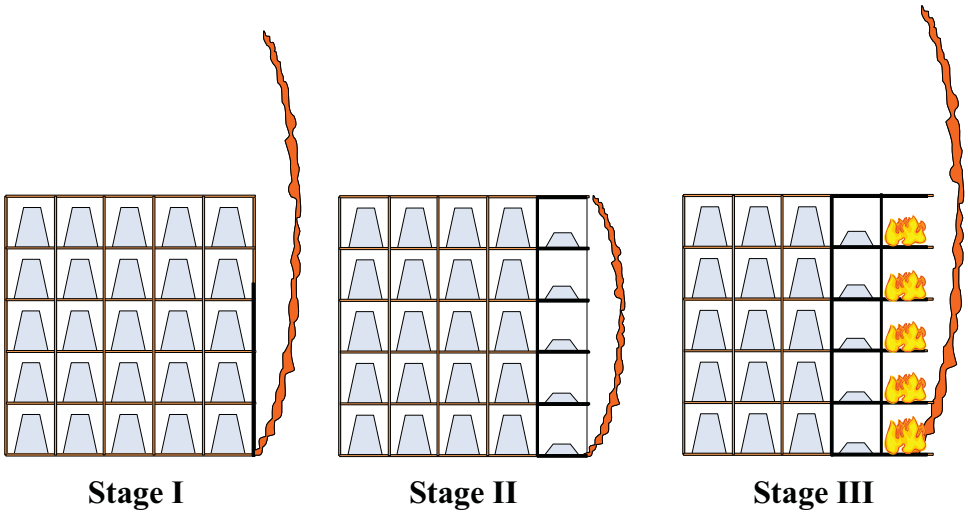

Figure 3: Side-view of the representative stages of burning for a Group A plastic commodity. Stage I on the far left consists only of upward flame spread along the outer corrugated cardboard face with no involvement of the inner packing commodity. Stage II in the center is the plateau region, where the inner packing material has mostly burnt away, starting to smolder and polystyrene is being heated before ignition resulting in a shorter fire plume. Stage III on the far right involves combustion of polystyrene and remaining cardboard from within the commodity.

can disintegrate, thereby exposing the commodity inside to direct flame impingement.

After the outer covering and inner packaging burn off, they smolder significantly slowing the burning rate as the inner plastic product heats toward its ignition temperature. This is described as stage II of burning, illustrated in figure 3. The plastic product (depending on its material properties) can then burn from inside or spill out as solid chunks or a viscous liquid pool once it reaches its ignition temperature, as illustrated in figure 2. At this later stage, the B-number is a function of the material properties of the corrugated cardboard, the commodity pyrolysis vapor (diffusing outward) and the commodity and packing material that have either spilled out or are burning within. This is referred to as stage III of burning for a standard plastic warehouse commodity, illustrated in figure 3.

5. Experimental Setup, Instrumentation and Procedure

The package tested was a single-walled corrugated cardboard carton of dimensions 530 $\times$ 530 $\times$ 510 mm that was compartmentalized by corrugated cardboard dividers with 125 basic products (in this case polystyrene cups) distributed within as seen in figure 4. The 6.25 kg package was 62% polystyrene and 38% corrugated cardboard by weight. The front face was made of approximately 3 mm thick single-ply corrugated cardboard with its flues oriented vertically. The package was wrapped in Kaowool insulating boards approximately 0.65 cm thick on all except one vertical side, on which measurements were taken. This arrangement, limiting the burning of the box, allows for a closer investigation of the fundamental physics governing the combustion of the plastic commodity.

The package was placed on top of a Setra, Super II load cell that measured the mass of the plastic commodity with an accuracy of ± 0.5 g. Figure 5 shows the experimental setup and instrumentation configuration. Inside the box 3 Type-K Chromel-Alumel thermocouples were installed inside five cells on the front face of the box. One set of thermocouples was placed on the front face of the corrugated cardboard to track the progression of the pyrolysis, one set was placed in the direct center of the cup to measure the temperature within the cup - nominally indicating the moment at which the cup ignites, and one set was hung to the side of a cup in the air space between the cup and cell wall - nominally indicating the cell's mean bulk temperature.

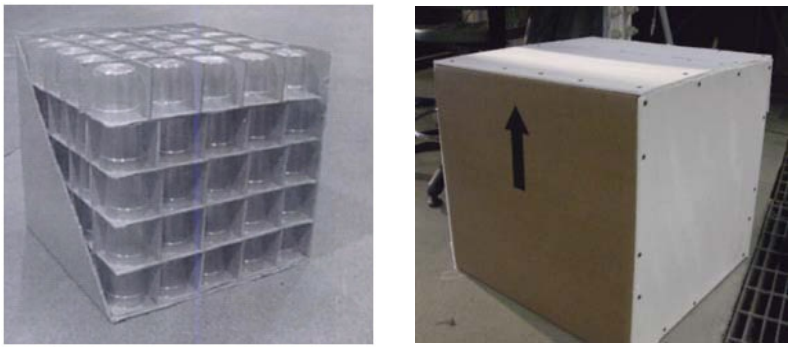

Figure 4: A Group A plastic commodity with half of its outer corrugated cardboard covering removed (left) [28] and with all but the front face insulated for experimentation (right).

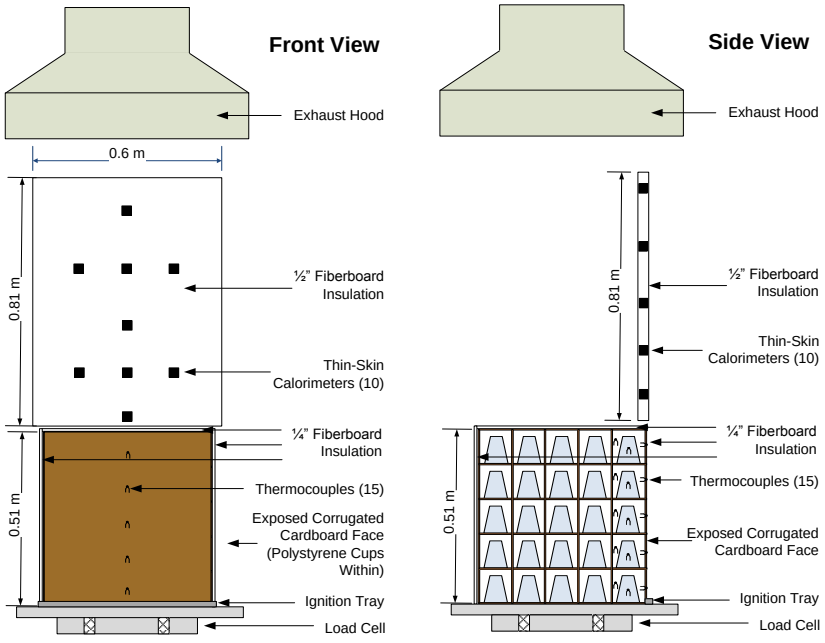

Figure 5: The experimental setup used to conduct tests on a standard Group A plastic commodity.

A Canon digital SLR camera was mounted on the side of the test apparatus to capture flame standoff distance. Time-stamped digital images were taken every five seconds, starting with ignition of the commodity. A Sony HD digital camcorder recording at 29.97 fps was positioned in front of the test apparatus to record flame heights and to visually compare the progression of the pyrolysis front.

Nine thin-skin calorimeters were mounted on a 1.3 cm thick, vertically oriented glass fiber board located above–and flush to the front face of the test commodity. This configuration allows for spatial measurements of the combined radiative and convective heat flux that the combusting plume of excess pyrolyzate will exert on stored commodities at higher elevation.

The setup was placed under a 1 MW hood to capture burning fumes and embers. Ignition was achieved by adding 4 mL of n-heptane to a strip of glass fiber board approximately 1 cm tall, 0.35 m wide by 3 mm in depth. The wetted wick igniter was held by an aluminum u-channel that was positioned adjacent to and below the lower front edge of the commodity. A National Instruments data acquisition card was used to record temperatures using Labview from thermocouples and thin-skin calorimeters. The video cameras and data acquisition program were started before ignition of the commodity. The data acquisition system and camcorders were synchronized with a stopwatch used to determine the offset between instrument start time and ignition start time. Experimental time begins when the strip is piloted at the centerline of the commodity's front face.

Due to safety concerns and to ensure instrumentation longevity, no tests were permitted to run past a point where material spillage occurs, as in figure 2. Once laboratory personnel decided this point was reached, a water spray was applied to extinguish flames.

6. Description of Fire History

Four tests were conducted, providing data on the mass-loss rate, heat flux, pyrolysis height, and flame height. Qualitative similarities between four conducted tests have produced a phenomenological description of the burning behavior of a standard plastic commodity. Selected frames from the camera placed in front of the burning commodity are shown for each of the three representative stages of burning in figure 6. Tests 2–4 were permitted to burn through all three stages, but test 1 was extinguished prematurely as extra caution was exercised in the first test. Three distinct stages of burning of the

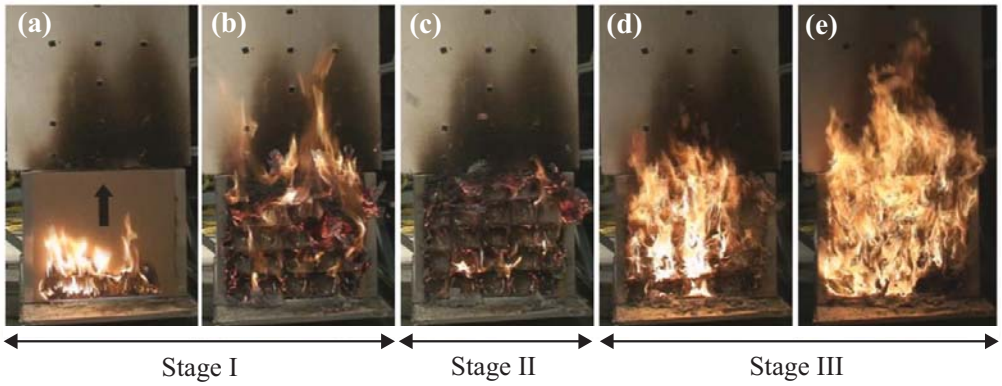

Figure 6: Representative test timeline: (a) 30 seconds, front layer pyrolyzing and time-dependent laminar burning along face, (b) 92 seconds, front face cells are exposed and burning, (c) 100 seconds, smoldering front face, second layer of cells being heated and polystyrene cups deforming, (d) 132 seconds, all cups in the first layer ignited and burning, (e) 150 seconds, second layer of cells also burning.

commodity can be identified from the observations, as illustrated graphically in figure 3.

Ignition of the corrugated cardboard containing a commodity may occur by piloted ignition with a wick, such as in the present experiments, or by radiant heating, as often occurs in the case of aisle-jumping in large-scale rack-storage configurations. The outer face of the commodity tested is made of two-layer corrugated cardboard. On the face where ignition occurs, the first layer will ignite and burn, eventually peeling away and igniting the second layer of corrugated cardboard, which will then experience a similar combustion process. The fire at this first stage is comparable to that of a single-ply sheet of corrugated cardboard burning upright. The arrangement of the commodity within the box has not yet influenced the burning. Figure 3 indicates that the stored plastic product is not yet involved in the burning. In a small percentage of commodities tested the polystyrene was observed to melt onto the second layer of corrugated cardboard which delays this layer from peeling away, reducing the initial burning rate.

For this typical commodity, the contents of the boxes burn sequentially as individual cells. Each cell is contained by corrugated cardboard on six sides with a polystyrene cup in the center as indicated in figure 3. While the front face of corrugated cardboard is burning, the first layer of cells be-

gins to be heated, and the corrugated cardboard within the cells close to the front face begins to pyrolyze. As soon as the corrugated cardboard front face peels away, oxygen can reach the smoldering corrugated cardboard in the cell, causing it to ignite quickly. Adjacent cells heat one another, and in this manner the entire front layer of cells ignites, although the polystyrene is not yet affected very much. Once the flaming combustion of corrugated cardboard within each cell in the first layer nearly ceases the commodity reaches the plateau stage of burning, shown in figures 6 and 3 labeled as stage II. During this plateau region cardboard smolders and cups absorb heat and are deformed until reaching the ignition temperature of polystyrene. Once the polystyrene reaches this temperature it ignites and begins to melt vigorously. The period of burning of the polystyrene cups is labeled in figure 6 and 3 as stage III. The melting and dripping of the polystyrene cups after their ignition, and the associated increased rate of heat flux from combustion of volatile polystyrene causes the second layer of cells to ignite and to repeat the process. As further layers of cells ignite, they add to a "wall" of flame formed by the dripping polystyrene and charred cardboard that moves inwards sequentially through layers of cells in the package.

7. Quantitative Results

Measurements of the mass lost over time are shown in figure 7. Transitions between stages that are indicated in the figure were deduced with the help of the data from the thermocouples that were suspended within cardboard cells and polystyrene cups. Air currents resulting from the turbulent combustion process create fluctuations in the mass-loss readings on the order of 1–3 grams. These small fluctuations, which are not representative of the actual mass loss, are smoothed over by applying polynomial fits to mass-loss data, resulting in the curves that are shown in figure 7 along with the raw data. In all cases fits with polynomials of different values were tried, and the order was selected that best reproduced all data, as judged by subjective visuals observations of the fits. Regardless of the selection, results produced were quite similar. Tests 1 and 2 were fit with 7th and 10th order polynomials, respectively. A ten-second section of test 2 in stage III was neglected because a piece of cardboard fell off the test sample then back onto the load cell, and all of stage II in test 4 was neglected because of behavior inconsistent with all other tests, probably because of large air-current fluctuations during this irregular burning period causing erratic load-cell readings. The first portion

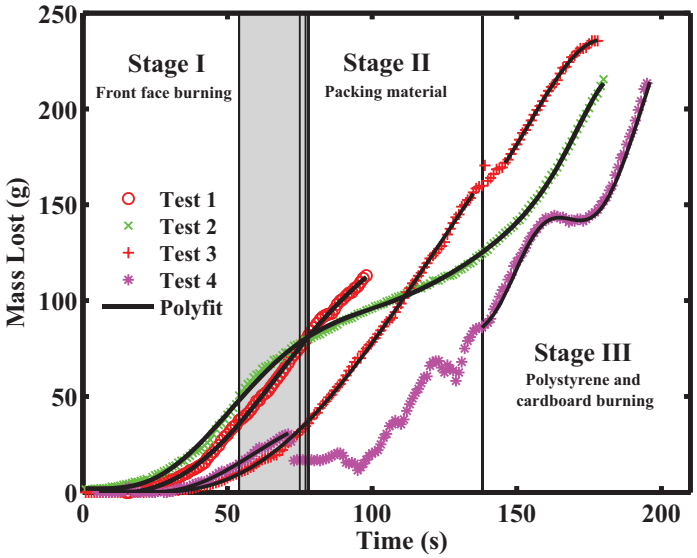

Figure 7: Mass lost from the commodity as a function of time, measured by a load cell at the base of the commodity. Polynomials are fit to the mass-loss measurements to smooth 2–3g fluctuations caused by air currents, but the smoothed data still captures the mixed commodity burning behavior. Relative stages of burning are indicated in the figure, with vertical lines denoting transitions between stages. The time line for each test was shifted so that the transition between stages II and III occurred at 138 seconds[1]. The deviations in time for the transition between stage I and II for the four different tests is indicated by the vertical gray band between those stages.

of tests 3 and 4 shown in figure 7 were fit with a 5th order polynomial, and 3rd and 7th order polynomials were used to fit the last portion of tests 3 and 4, respectively. The transition between stages I and II, chosen as the point where inner packing material starts to burn and upward flame spread has reached the top of the front face of the package, or is close to the top, occurs around 77 seconds for three of the four tests. The inclusion of test 4, which displays an earlier transition between stages I and II, is useful for indicating the range of deviations that may occasionally occur in complex tests such as these; the dips in the curve in this run are associated with burning material becoming detached then landing on the scale.

The mass-loss rate was calculated from the derivatives of polynomial fits of recorded mass lost over time. Fluctuations in the mass-loss rate occur because of both time-dependent changes in the material burning and changes

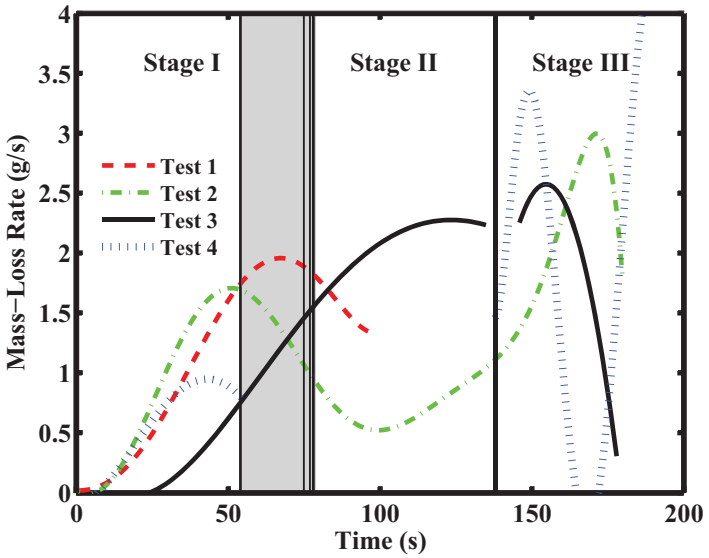

Figure 8: Mass-loss rates, calculated from the derivative of polynomial fits to the mass-lost data. Relative stages of burning are indicated in the figure as described in the caption of figure 7.

in the mixture of constituents burning throughout the box over time, and the error is estimated to be on the order of ± 0.05 g/s. The mass-loss rate shown in figure 8 steadily increases during most of stage I as the flame front progresses over the front face. The mass-loss rate then slows and tends to reach a plateau at the beginning of or during stage II while corrugated cardboard packing material burns and polystyrene melts and gasifies. The mass-loss rate then typically decreases as all remaining corrugated cardboard burns out. Once polystyrene reaches its ignition temperature at the beginning of stage III, the mass-loss rate sharply increases, until water spray is applied to extinguish the flames.

The heat flux to a vertically oriented surface above the tested commodity, measured by thin-skin calorimeters, is shown in figure 9. The heat flux was determined by applying a 7-point moving average to temperature histories

[1]Because of the variability of the ignition procedure and the irregularity of the initial small flames, it was difficult to define exactly when the ignition occurred, but this was estimated to occur at 28s, 0s, 6s, and 1s for tests 1, 2, 3, and 4, respectively, in figure 7.

of the sensor element of the thin-skin calorimeters measured at 10 Hz. This serves to smooth the data while still giving a time resolution better than 1 second, much finer than that of the load cell and meaningful because this is nearly a point measurement, rather than being integrated over the entire volume of the fire. A finite-difference formula was applied to this data to determine its derivative. The heat flux was calculated accounting for radiative, convective, and storage losses using a method outlined by ASTM E 459-97 [29]. The heat fluxes displayed in figure 9 represent a combined radiative and convective heat flux at this higher elevation. They are not equatable to the heat flux directly in front of the commodity, but they can be used for analysis of upward spread rates. These heat fluxes sharply increase toward the end of stage I of burning, unlike the mass-loss rate which steadily increases throughout the first part of stage I. The high peak heat flux observed after approximately 1 minute of burning is likely to contribute to the rapid upward flame spread rates seen in large warehouse fires. The heat flux then steadily declines throughout the burning- rate plateau of stage II, and it increases again with the involvement of polystyrene in stage III.

Ranges of flame heights, determined from high-definition camcorder recordings of images of the front of the commodity are shown in figure 10. Images were first imported into ImageJ [30], converted into gray scale, and passed through a 3×3 Sobel edge-detection algorithm provided with the software. Traces of the edge of the observed yellow flame were confirmed visually, and the highest points of attached flames selected from the peak of the traces were to define the maximum flame height. An alternative method of determining flame heights, thresholding, was also applied to the data but was found to decrease the accuracy of measurements for a number of reasons. Flame brightness grew considerably throughout the test, requiring repeated changes in the exposure level of the lens in order to observe the flame for the entire duration. In contrast to other work [31, 32], a constant threshold was therefore not appropriate, and despite efforts to develop a method that subtracted background noise and adjust threshold levels with ambient brightness, it was not possible to compensate for background changes, such as soot deposition on the inert wall above the setup, throughout the test duration. Highlighting jumps in intensities between adjacent pixels, i.e. edge detection, was found to be more appropriate for this series of tests, coupled with visual confirmation that the highlighted region was in fact the attached yellow flame. Analysis of some tests with a constant threshold of 0.6 (with 0 representing black and 1 white) did reveal a trend similar to the heights

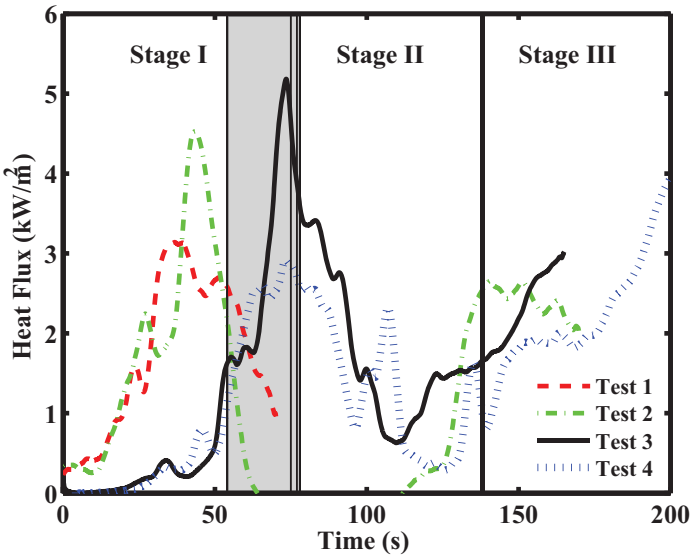

Figure 9: The heat flux measured by a vertically oriented thin-skin calorimeter approximately 3 cm directly above the top center of the face of the tested commodity, representing a combined convective plus radiative heat flux exerted on commodities at higher elevations. Relative stages of burning are indicated in the figure, as described in the caption of figure 7.

presented in figure 10, and all such results are encased within the gray error bands.

As flame heights fluctuate widely during turbulent combustion, the range of observed maximum flame heights are indicated in figure 10 by a gray band, and a smoothed average of values is indicated by a solid line in the center of the shaded region. It is possible to repeat a similar procedure across the width of the flame front during stage I, calculating the average value of the maximum flame height across the width during a particular time step. This resulting average flame height is perhaps more representative of the combusting plume region ($X_f - X_p$) than the maximum flame height because it represents the average area of virgin material heated by the flame, rather than just a maximum height which represents some decaying heat flux to the fuel surface. This average flame height has been calculated during early stage I combustion in these tests, and approximately rests along the minimum of the gray error band. As expected, the average flame height across the front face is lower than the maximum flame height, although preliminary results indicate the flame height also increases at a slower rate than does the maximum flame height.

The location of the pyrolysis front was also determined from video footage, defined as the location where brown corrugated cardboard blackens due to charring. The average location of this front, determined from averaging the maximum front position visually across the front face was used to determine the front location. The pyrolysis height may alternatively be derived from temperature readings of thermocouples mounted along a column of cells in the front face of the commodity. Recorded thermocouple temperatures of 380 °C, the ignition temperature of cellulose reported in literature [33], were chosen to mark the locations of the pyrolysis front. Approach to a temperature plateau in thermocouple data is an alternative criterion, but this was found to occur within 5 °C of 380 °C. At any given time, the resulting heights from the thermocouple measurements were only about half those obtained from video footage. These deviations between thermocouple data and visual observations of charring suggest there were delays between the pyrolysis front reaching the thermocouple location and subsequent heating, potentially caused by gaps between the solid fuel and thermocouples or significant heat loss by conduction along the thermocouple wires. Therefore, video data was thought to provide the most reliable source of pyrolysis height data, presented in figure 10. Gray bands are used to indicate experimental spread between tests.

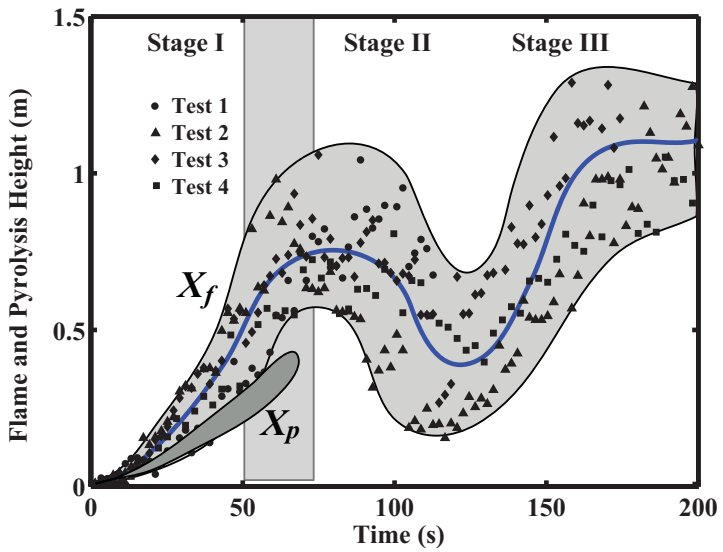

Figure 10: Ranges of maximum flame (X_f) and average pyrolysis (X_p) heights from four tests, with gray bands between the curves indicating experimental scatter, in that all experimental points (symbols) lie within the gray bands. The line in the middle of the band is the average of all of the data points. Relative stages of burning are indicated in the figure, with vertical lines denoting transitions between stages, as described in the caption of figure 7.

In figure 10, the pyrolysis height pertains only to stage I because at the end of that stage, the pyrolysis front has reached the top of the package. The flame heights, however exhibit the same three stages as the mass-loss rate and heat flux shown in figures 8 and 9. Flame heights rapidly increase during initial burning, reflecting the high fire hazard of outer corrugated cardboard covering. They then taper off as the cardboard begins to smolder. The decrease in flame heights corresponds to smoldering of packing material and to a decrease in the excess pyrolyzate burning above the tested commodity. A steady increase in flame height is observed once volatile polystyrene reaches its ignition temperature and dominates the burning process in stage III. The fact that the burning is more vigorous in stage III than in stage I, due to the involvement of more fuel, reflected in the higher mass-loss rate in stage III seen in figure 8, increases the excess pyrolyzate and causes more of the heat release to occur at higher elevations, moving the flames away from the thin-skin gauges, thereby tending to decrease their readings, as seen in figure 9. A more detailed presentation of collected data, including thermocouple traces is available in a reference [34].

8. Extraction of B-number Values

Equation 7 was used to determine a B-number as a function of time using the experimentally determined mass-loss rates shown in figure 8. Recently, time-dependent B-numbers were addressed by Pizzo et al. [24] for laminar upward flame spread over small polymethyl methacrylate slabs. In the present work, larger fluctuations are experienced due to turbulence, the mixed nature of the commodity and its more complex geometry. In calculating B, the values [25] ρ_g =0.50 kg/m^3, $\alpha_g = 9.8 \times 10^{-5}$ m^2/s and $\nu_g = 6.8 \times 10^{-5}$ m^2/s were used. A mean gas temperature, T_g for use in the calculation was found by averaging the temperature of ambient gas, $T_\infty = 20\,^\circ$C and an approximate flame temperature for cellulosic materials, $T_f = 800\,^\circ$C [23, 35].

The area of burning during stage I was calculated from visual video measurements of the blackened pyrolysis region on the front face. Video measurements of the blackened pyrolysis front across the width of the front face were taken to determine the area burning throughout the first stage. A second-order polynomial was found to fit well with the area measured in the video for each test, for the purpose of calculating $\dot{m}''_f$ in equation 7 for stage I. This area increases steadily over time, reaching a maximum value between 54 to 77 seconds (the end of stage I for the respective test). A constant

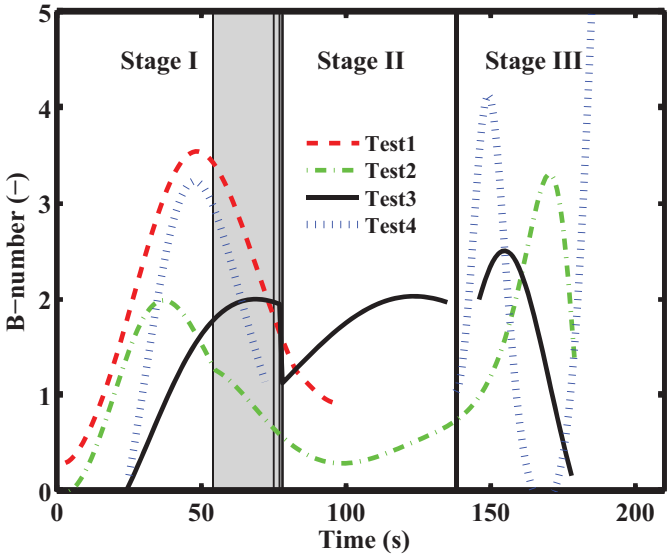

Figure 11: Time-dependent B-numbers calculated from the mass-loss rate using equation 7. The B-numbers in stage I were calculated using a varying area of burning, while the area was taken constant in stages II and III. Relative stages of burning are indicated in the figure, with vertical lines denoting transitions between stages, as described in the caption of figure 7.

area equal to the total area of the front face of the package was assumed for calculating $\dot{m}''_f$ during stages II and III. During stages II and III there are variations in the exposed burning surface areas of the packing material and of the commodity, but these areas cannot be estimated well, and on the average the total burning surface area in these stages is approximately the total front-face area. Because the initial burning area cannot be determined in stages II and III, uncertainties in B at any given time on the order of a factor of two must be accepted so that the resulting time dependence of B is at best qualitatively indicative of its variations during these later stages. The first 15-20 seconds of all measurements are neglected to remove effects of the ignition source. The resulting time-dependent B-numbers of the four tests are shown in figure 11, in which the most reliable time dependencies pertain to stage I.

With these procedures, in stages II and III the calculated variations of B are proportional to the variations of the mass-loss rate seen in figure 8. In stage I, however, the increasing area causes the variations in B to exceed

those of the mass-loss rate. Comparisons of figures 8 and 11 shows that the result is that the values of B tend to vary over roughly the same range in all three stages, while the mass-loss rate is clearly much smaller during the early part of stage I than during the later stages. While significant deviations in the time-dependent B-number exist, just as for the mass-loss rate, the subsequent average values of B for each stage vary much less, as can be inferred from figure 11.

The time-dependent B-number in stage I reaches a peak toward the end of the stage as the pyrolysis front accelerates upward, consistent with the increasing heat flux from the flame, shown in figure 9. The B-number then decreases as the cardboard smolders in stage II, where the pyrolysis front has reached the top of the front face, reducing the amount of excess pyrolyzate and thus the applied heat flux. In some cases this is different from the mass-loss rate in figure 8 for stage I, where it is seen that for test 3 the mass-loss rate nearly constantly increases throughout stage I and into stage II, underscoring the general variability of the fire development. Stage III presents even more varied behavior as the ignition of polystyrene cups in each test occurs in a different pattern, but all show very steep increases in the B-number, just as in the mass-loss rate. Stage III introduces additional uncertainties associated with using a constant area of burning because polystyrene melts and drips, increasing its burning surface area, and it is difficult to accurately determine the processes involved during such a dynamic stage.

Rangwala et al. [27] found that an experimentally determined B-number changes over time for a material, and they suggested a method of averaging the B-number over time. Applying their method, a time-averaged B-number for each of three stages was found by time-averaging the mass-loss rate per unit area in each stage, and using this value to calculate an average B-number of the stage. Values of B averaged for each relative stage of burning, reflecting the average burning rate for that stage are given in table 2. While a number of other averaging methods can be defined, such as averaging directly over time in figure 11, the results are not substantially different. These B-numbers do no more than reflect relative burning rates and include substantial simplifications, especially in stages II and III via a constant burning area assumption, that means they should not be used for more than relative comparison. In fact, within the error limits of the B-number calculation the values are the same in stages I and III.

Average burning rates, $\dot{m}_{f,avg}$ in table 2 were determined by averaging mass-loss rates from figure 8 for each stage, and taking the average of these

Summary of Stages			
Stage I	Outer layer of commodity is ignited, producing rapid upward turbulent flame spread over the front face of a commodity. B is independent of polystyrene.	$\boldsymbol{B_{avg}}$	**1.8**
		$\dot{m}_{f,avg}$	0.83 g/s
		$X_{f,max}$	0.51 m
		$\dot{q}_{f,avg}$	1.2 kW/m^2
Stage II	Front layer of corrugated cardboard has burned to top, exposing inner region, which burns and then smolders. Polystyrene does not burn because of its higher ignition temperature.	$\boldsymbol{B_{avg}}$	**1.4**
		$\dot{m}_{f,avg}$	1.7 g/s
		$X_{f,max}$	0.48 m
		$\dot{q}_{f,avg}$	0.38 kW/m^2
Stage III	Polystyrene ignites and a rapid increase in the burning rate occurs.	$\boldsymbol{B_{avg}}$	**1.9**
		$\dot{m}_{f,avg}$	2.2 g/s
		$X_{f,max}$	0.65 m
		$\dot{q}_{f,avg}$	2.4 kW/m^2

Table 2: Summary of burning behavior over 3 representative stages for a standard plastic commodity. Note that values are taken as either the indicated maximum or average in the denoted region for each test, and then averaged for all four tests. The average and peak heat fluxes given here were measured by a thin-skin calorimeter 3cm directly above the test commodity, indicating the heat flux applied to material directly above the commodity.

values for all four tests. The mass-loss rates, independent of burning area, increase from stages I-III, growing as the amount of material burning increases, and in stage III they increase as volatile polystyrene becomes the primary material burning.

The B-number for stage I is markedly higher than it would have been if it were calculated using a non-varying area, because the small area of burning during the initial stages of upward spread dramatically increases the value in that calculation, shown in figure 11. The average B-number of each stage of burning is influenced by the mixture of constituent materials involved in combustion during that stage. In stage I, the burning rate is solely dependent on corrugated cardboard combustion, resulting in a B-number of 1.8. If it is assumed that the area of burning in stages II and III is the front face of the commodity, reasonable for comparison because this is the area exposed during a warehouse fire, the B-number decreases to 1.4 for stage II. In stage II, this sensible decrease occurs due to smoldering of burnt material and heating of polystyrene. The B-number for stage III, 1.9 cannot be differentiated from that of stage I within experimental error, even though it is influenced by the combustion of polystyrene and cardboard together. What can be inferred

from this data, within reasonable experimental error is that the intensity of burning between stages I and III may be similar, but because stage III has a much larger burning surface area that steadily burns for a long period of time stage III is considerably more hazardous than stage I in terms of overall burning rate and flame heat flux.

Maximum flame heights observed from the videos were averaged from all four tests to give the values of $X_{f,max}$ for each stage listed in table 2. The highest flame heights were observed during stage III, where volatile polystyrene burns at the highest B-number, producing additional excess pyrolyzate lifting the flames higher above the test apparatus. The flame height is noticeably shorter in Stage II, on average, because the smoldering of cardboard packing material slows down the burning process. Maximum flame heights observed in test I as flames accelerate up the face are greater than those observed in stage II, although earlier in stage I flame heights are smaller.

Peak heat fluxes above the commodity for each stage, averaged from all four tests, achieve their highest values in stages I and III, similar to the flame heights as seen in table 2. Heat fluxes above the commodity peak substantially higher in stage III than in stage I, double the value, and are significantly lower in stage II than in stage I, one third the value. These sharp deviations occur because smaller increases in the burning rate significantly increase the amount of excess pyrolyzate burning above the front face of the commodity, thereby increasing the rate of heat release and thus heat flux to think-skin calorimeters mounted above the commodity.

9. Discussion of Results

The "practical," experimentally measured average values of B given in table 2 can be compared to theoretically calculated thermodynamic values for both corrugated cardboard and polystyrene by using equation 1 and assuming χ and Q equal zero [15] to obtain an ideal value, assuming there are no losses. Annamalai and Sibulkin [33] report values of heats of combustion and heats of vaporization which when used provide B-numbers of 6.4 and 1.6 for cellulose and polystyrene, respectively. The value for cellulose is, however, not representative of practical cellulosic materials; it is much too high because the heat of gasification is too low. Tewarson [36] reports a heat of gasification for corrugated cardboard, which results in $B = 1.1$ instead, a more reasonable value. The calculated ideal value of 1.6 for polystyrene is consistent with results obtained from other literature [36, 37]. It may be

concluded that the thermodynamic values of B for these two materials do not differ greatly, both lying between 1 and 2, with the values for polystyrene somewhat higher than the other. The values in table 2 are also in this range, although slightly higher in stages I and III. The difference between the thermodynamic and experimental values is hard to distinguish because of experimental error, but their similar magnitudes suggest that the present results are reasonable. More accurate experimental measurements should reflect real-world heat-transfer processes, notably radiative feedback, which can cause Q to be negative in equation 1.

The determination of a B-number of mixed materials would be a useful step toward characterizing the flammability of mixed materials, with potential future applications for warehouse commodity classification. A theoretical exercise can be performed to demonstrate this possibility, though errors preclude use of the result, at least at present. The B-number of stage III would be expected to be some combination of corrugated cardboard and polystyrene, creating a "composite" B-number for the stage. One approach would be to combine the influence of material constituents by weight percent. Combining the B-numbers of corrugated cardboard and polystyrene by weight percent results in a composite B of 1.4 if thermodynamic values are used (1.1 for corrugated cardboard and 1.6 for polystyrene). In obtaining this result, the product mass percent was calculated from the total weight of the Group A commodity, 2.38 kg corrugated cardboard and 3.88 kg polystyrene. Another possible combination could be weighted by the exposed burning surface area, which results in a combined thermodynamic B-number of 1.2 when the exposed surface area is defined as the area exposed in the first layer of cells, not including the front face which burned away, so the area of exposed polystyrene is taken to be 0.296 m^2, and corrugated cardboard 0.944 m^2. Both of these estimates produce values of B lower than the experimentally measured value for stage III, although the result is well within error bounds. The value of B for corrugated cardboard measured experimentally is the same as the theoretical value for polystyrene, within experimental error, so any combination using this value and the thermodynamic value of B for polystyrene would be the same, and thus it is inconclusive for testing how best to estimate a value for mixed materials.

While the "predicted" values of B in table 2 lie between 1 and 2, fluctuations in values between 0 and 5 are seen to occur in figure 11. Only by averaging over these large fluctuations can values be obtained that are potentially useful for commodity classification. The relatively small range of

the averaged values suggest the possibility of selecting values representative of mixed materials that can be helpful in hazard assessment. Qualitative results from these experiments suggest an approach to determining such values may be accomplished by separate tests of combined materials, i.e. corrugated cardboard alone for stage I and cardboard and polystyrene together for stage III. Experiments in such a configuration may prove insightful, provided the geometry is simple enough to allow similar behavior over a large number of tests.

The determination of a B-number of mixed materials has potential for use particularly in warehouse commodity classification, serving as a measure of the mixed material's thermodynamic driving force, or relative intensity of burning. Experiments have shown distinctively separate behavior in each stage of burning, although errors in this complex test setup have hindered the potential drawing of useful conclusions. Still, if a methodology is accomplished that can determine such a parameter to within acceptable error bounds, this thermodynamic driving force can be used to estimate the thermal loading of a potential fire, and thus be used to rank commodities against one another and assist in the design of suppression measures.

It is to be noted that this test setup presents many obstacles to determine an accurate B-number. The surface is wide which allows horizontal flame spread as well as buoyancy-induced vertical spread. Deviations in the front face of corrugated cardboard as well as varying influences of materials within the commodity during upward flame spread present many difficulties in this test setup. Careful observations of the test results must be conducted in order to reject regions of non-upward flame spread during this test, as well as other deviations such as chunks of material falling off the test stand. Despite the difficulties of this test setup, it has yielded relevant information on general fire behavior, ranges of values of B to be expected and on the incremental stages of burning which occur within the commodity. More accurate smaller-scale tests should be conducted as research continues.

10. Conclusion

This work has provided preliminary data on a new method to experimentally measure B-numbers of a mixed material configuration. Small-scale tests performed on a Group A plastic commodity were used to calculate time-dependent as well as time-averaged values of the B-number for each of the three distinct stages of burning that were found in the present tests.

Because a Group A plastic commodity is mixed, consisting of plastic and corrugated cardboard products, each of the three stages is dominated by a different combination of constituent materials. Significant hazards known to occur in warehouses due to upward flame spread have been addressed here, with measurements of heat fluxes, observations of rapidly increasing flame heights, and calculations of larger B-numbers immediately after ignition of the commodity and during the combustion of the plastic product. During an intermediate stage a decrease in the burning rate is observed as transition to the plastic burning process begins. The experimental B-numbers reported here contain inaccuracies, and although the results experimentally incorporate more physical processes than analytically determined thermodynamic B-numbers, the final values are not very different, within experimental error. Use of this approach to assess the flammability of mixed materials will require additional work that includes some large-scale testing and smaller scale experimentation over a large number of samples, so that average behavior can be assessed.

11. Acknowledgments

We are grateful to Garner Palenske, Vice President, Schirmer Engineering Corporation, San Diego, California for providing funding for this study and David LeBlanc, Director of New Technology, Tyco Fire Suppression and Building Products, Cranston, Rhode Island for donations of the commodity used in these experiments. The authors would like to acknowledge the assistance of Todd M. Hetrick, graduate student, Worcester Polytechnic Institute (WPI), and Cecelia Florit (undergraduate summer exchange student, University of Marsielle, France) for their contributions to the laboratory experiments. Assistance from WPI laboratory manager, Randall K. Harris is also appreciated. We would also like to thank the three reviewers who provided detailed comments that significantly improved the presentation of this work, and we are grateful for valuable discussions with Professor Jose L. Torero, University of Edinburgh, UK.

12. References

[1] L. Nadile, "The problem with big," *NFPA Journal*, March/April 2009.

[2] clicktohouston.com, "Fire destroys Houston furniture warehouse." May 22, 2009.

[3] T. R. Merinar, "Nine career fire fighters die in rapid fire progression at commercial furniture showroom - South Carolina," Fatality assessment and control evaluation (FACE) investigation report. No. F2007-18, National Institute for Occupational Safety and Health, 2009.

[4] L. Frederick, J. L. Tarley, C. Guglielmo, and T. Merinar, "Career fire fighter dies of carbon monoxide poisoning after becoming lost while searching for the seat of a fire in warehouse - New York," Fatality assessment and control evaluation (FACE) investigative report. No. F2004-04, National Institute for Occupational Safety and Health, 2005.

[5] National Fire Protection Association, "Fire investigation report: supermarket - Phoenix, Arizona (March 14, 2001)," tech. rep., National Fire Protection Association.

[6] F. Washenitz, K. Cortez, T. Mezzanotte, M. McFall, T. Merinar, T. McDowell, and V. Dunn, "Warehouse fire claims the life of a battalion chief - Missouri," fatality assessment and control evaluation (FACE) investigative report. No. 99-F48, National Institute for Occupational Safety and Health, 2000.

[7] R. W. Braddee, T. R. Merinar, T. P. Mezzanotte, T. Pettit, N. T. Romano, and F. C. Washenitz, "Six career fire fighters killed in cold-storage and warehouse building fire - Massachusetts," Fatality assessment and control evaluation (FACE) investigative report. No. 99-F47, National Institute for Occupational Safety and Health, 2000.

[8] NFPA, "NFPA fire investigations report, bulk retail store fire, Albany, GA, April 16, 1996," tech. rep., National Fire Protection Association, Quincy, MA. 1997.

[9] R. G. Zalosh, *Industrial Fire Protection Engineering.* John Wiley & Sons, New York, 2003.

[10] R. K. Dean, "A final report on fire tests involving stored plastics," *Fire Technol.*, vol. 12, no. 1, pp. 55–65, 1976.

[11] Factory Mutual Insurance Company, *FM Global Property Loss Prevention Data Sheet 8-1*, 2004.

[12] H. Ingason, *Experimental and Theoretical Study of Rack Storage Fires*. PhD thesis, Lund University, Institute of Technology, 1996.

[13] M. Foley, *The use of small scale fire test data for the hazard assessment of bulk materials*. PhD thesis, University of Edinburgh, 1995.

[14] P. J. Pagni and T. M. Shih, "Excess pyrolyzate," *Proc. Combust. Inst.*, vol. 16, pp. 1329–1343, 1977.

[15] J. L. Torero, T. Vietoris, G. Legros, and P. Joulain, "Estimation of a total mass transfer number from the standoff distance of a spreading flame," *Combust. Sci. Technol.*, vol. 174, no. 11, pp. 187–203, 2002.

[16] H. W. Emmons, "The film combustion of liquid fuel," *Zamm-Z. Angew. Math. Me.*, vol. 36, 1956.

[17] A. S. Rangwala, *Flame spread analysis using a variable B-number*. Phd thesis, University of California, San Diego, La Jolla, CA, 2006.

[18] K. Annamalai and M. Sibulkin, "Flame spread over combustible surfaces for laminar flow systems Part II: Flame heights and fire spread rates," *Combust. Sci. Technol.*, vol. 19, no. 5, pp. 185–193, 1979.

[19] D. J. Holve and R. F. Sawyer, "Diffusion controlled combustion of polymers," *Proc. Combust. Inst.*, vol. 15, no. 1, pp. 351 – 361, 1975.

[20] T. Ahmad and G. M. Faeth, "Turbulent wall fires," *Proc. Combust. Inst.*, vol. 17, pp. 1149–1160, 1978.

[21] D. J. Rasbash, "The extinction of fires by water sprays," *Fire Res. Abst. Rev.*, vol. 4(1), no. 28–53, 1962.

[22] A. M. Kanury, *Introduction to Combustion Phenomena*. Gordon & Breach Science Publishers, New York, 1975.

[23] C. K. Law and F. A. Williams, "Kinetics and convection in the combustion of alkane droplets," *Combust. Flame*, vol. 19, pp. 393–405, 1972.

[24] Y. Pizzo, J. L. Consalvi, and B. Porterie, "A transient pyrolysis model based on the B-number for gravity-assisted flame spread over thick PMMA slabs," *Combust. Flame*, vol. 156, no. 9, pp. 1856–1859, 2009.

[25] P. J. DiNenno, ed., *SFPE Handbook of Fire Protection Engineering, Fourth Edition*. National Fire Protection Association, 2008.

[26] F. P. Incropera and D. P. DeWitt, *Introduction to Heat Transfer*. John Wiley & Sons, New York, 1996.

[27] A. S. Rangwala, S. G. Buckley, and J. L. Torero, "Analysis of the constant B-number assumption while modeling flame spread," *Combust. Flame*, vol. 152, no. 3, pp. 401–414, 2008.

[28] A. E. Cote, *Operation of fire protection systems: a special edition of the Fire Protection Handbook*. Jones and Bartlett Publishers, National Fire Protection Association, 2003.

[29] ASTM, *Standard Test Method for Measuring Heat Transfer Rate Using a Thin-Skin Calorimeter*. ASTM, West Conshohocken, PA, test standard ed.

[30] W. Rasband (NIH), "ImageJ." http://rsb.info.nih.gov/ij/, 2006.

[31] L. Audouin, G. Kolb, J. L. Torero, and J. M. Most, "Average centreline temperatures of a buoyant pool fire obtained by image processing of video recordings," *Fire Saf. J.*, vol. 24, no. 2, pp. 167–187, 1995.

[32] Y. Pizzo, J. Consalvi, P. Querre, M. Coutin, L. Audouin, B. Porterie, and J. Torero, "Experimental observations on the steady-state burning rate of a vertically oriented pmma slab," *Combustion and Flame*, vol. 152, no. 3, pp. 451–460, 2008.

[33] K. Annamalai and M. Sibulkin, "Flame spread over combustible surfaces for laminar flow systems Part I: Excess fuel and heat flux," *Combust. Sci. Technol.*, vol. 19, no. 5, pp. 167–183, 1979.

[34] M. J. Gollner, "A fundamental approach to commodity classification," Master's thesis, University of California, San Diego, La Jolla, CA, January 2010.

[35] J. G. Quintiere, *Fundamentals of Fire Phenomena*. John Wiley & Sons, New York, 2006.

[36] A. Tewarson, "Sfpe handbook of fire protection engineering, fourth edition," ch. Generation of Heat and Gaseous, Liquid, and Solid Products, pp. 3–(109–194), National Fire Protection Association, 2008.

[37] P. J. Pagni, "Diffusion flame analyses," *Fire Saf. J.*, vol. 3, no. 4, pp. 273–285, 1981.